A Novel Hybrid Approach for Wireless Powering of Biomedical Implants

Mehdi Kasaee Kopaei[#1], Arash Mehdizadeh[#2], Damith C. Ranasinghe[*3], Said Al-Sarawi[#4]

[#] *Centre for Biomedical Engineering,* [‡]*School of Electrical and Electronic Engineering,*

[*]*Auto-ID Lab, School Computer Science,*

The University of Adelaide, Adelaide, SA 5005, Australia

[1]mehdika, [2]arash, [4]alsarawi@eleceng.adelaide.edu.au

[3]damith@cs.adelaide.edu.au

***Abstract*—Harvesting adequate power for actuation in implanted biomedical devices using an electromagnetic field is a challenging task. Previous attempts to actuate and control deep implants have proven difficult and challenging. In this paper we propose an alternative solution to remote powering and actuation of implanted biomedical devices using a novel hybrid magneto-electric energy harvesting approach. This new approach with the possibility for secure operation is demonstrated in this paper through a (Micro-Electro-Mechanical Systems) MEMS device. We have conducted an analytical and finite element model using ANSYS for the proposed power transfer system to confirm that adequate power can be transferred to operate a MEMS based biomedical device. We have shown that our proposed approach is able to generate 1.3 V under shear stress and provides adequate voltage to successfully operate a micropump. Our numerical results indicate directional actuation of an electrostatically actuated diaphragm of a mechanical micropump up to 1.8 μm resulting in a stroke volume of 10% of the total volume of the chamber.**

I. Introduction

By developing implantable biomedical devices such as drug delivery micropumps, smart stents, RF MEMS switches and diagnostic monitoring systems, research on powering and prolonging the lifetime of power source for these electronic devices has become more significant. Unlike everyday consumer portable devices, it is not possible for implanted devices to recharge or replace their power source regularly since the battery replacement would be risky and expensive [1]. The importance in such cases has been on developing the onsite energy harvesting system that can convert accessible forms of human body energy into electrical and in turn, other forms of energy.

Nowadays much research has been focused on harvesting energy from environmental energy sources. Energy harvesting may be based on several sources. In the case of Bio-MEMS and implantable biomedical devices, mechanical vibration is potentially a first source of power accessible in the human body. These vibrations could further be generated by an external power source such as oscillating magnetic fields. Conversion of mechanical vibrations into electrical energy is feasible by electrostatic, electromagnetic and piezoelectric transducers; each of which has its own advantages for certain applications. Nevertheless, due to the higher energy density and actuation capability, piezoelectric transducers are more favourable [2-4].

A significant amount of research has been devoted to developing an efficient power harvesting system based on piezoelectric transducers harvesting energy from body movements. In [5] a blood pressure source is considered to induce stress to a piezoelectric transducer. Their work compares 3-3 and 3-1 modes of operation for a piezoelectric generator using a PZT-5A membrane. The results from this work have demonstrated that the 3-1 mode or thin plate element has mechanical advantages in converting applied pressure. Moreover, this analysis confirms that an in vivo piezoelectric generator on size scale of 1 cm^2 is able to power a bio-MEMS application in the μW power range continuously.

PZT ceramics are suggested in [6] to generate sufficient energy within total knee replacement (TKR) implants to operate a low power microprocessor and accompanying sensors for diagnostic and monitoring applications. The results indicate that three PZT ceramic elements with total volume of 1.2 cm^3 embedded within TKR implants can generate 4.8 mW under expected axial loading conditions.

Energy harvesting techniques that utilize ambient sources of energy are not suitable for small-scale implants as miniaturization of harvesting devices leads to significantly reduced power and readily accessible ambient power sources do not exist within the human body [6, 7].

In contrast to power harvesting approaches, researchers in [8, 9] have shown how power can be transmitted wirelessly to medical implants. In another study researchers at Stanford [10, 11] demonstrated wireless power transfer to a millimetre sized device implanted five centimetres inside the chest on the surface of the heart. Results of this study show that mid-field wireless powering achieves much higher power compared to conventional inductively coupled systems. In addition with accurate system design, adequate power to activate typical cardiac implants can be harvested by millimetre sized coils.

In this paper we propose an alternative solution to remote powering and actuation of MEMS devices using a novel hybrid approach, which combines a magneto-electric energy harvesting MEMS device with a surface acoustic wave sensor using an input interdigitated transducer (IDT) to ensure the secure operation of the biomedical device. A new magneto-electro acoustic conversion system by utilizing piezoelectric

material is used in the energy harvesting module to convert mechanical energy provided by an oscillating magnetic field into electric power. In this system the piezoelectric material is coupled with a permanent magnet, which is then used to convert mechanical oscillations induced in the magnet to stresses induced in a slab of piezoelectric material resulting in an electric potential. In this paper we have conducted an analytical and finite element analysis using ANSYS for the proposed energy harvesting system to demonstrate that enough power can be harvested to activate an implantable biomedical device. The resultant electric potential is then used in a Finite Element Analysis (FEA) model of an electrostatically actuated diaphragm of a mechanical micropump to show the merit of the wireless powering technique for actuation of micro-implants.

II. A Hybrid Approach for Implants

Fig. 1 illustrates the secure wirelessly actuated MEMS device comprised of: i) a "secure interrogation module" which responds to an encoded frequency; ii) a micro switch; iii) micro medical device (such as a micro pump); and iv) a magnetoelectric energy harvester. Given that the frequency of the RF signal matches the IDT's, the harvested energy from the energy harvesting module transfers to actuate the MEMS device.

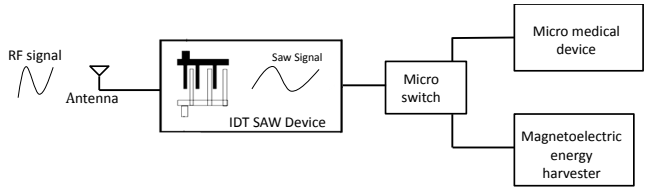

Fig. 1. Conceptual model of a secure wirelessly actuated biomedical device.

Secure interrogation module is extensively discussed elsewhere [12] and the focus in this work is on the energy harvesting module and its ability to generate adequate power to operate a micro medical device such as a micropump.

III. Magneto-Electric Energy Harvesting System

The concept outlined in this work relies on the induced mechanical forces that are generated by a large volume low frequency magnetic field around a piezoelectric crystal bonded with a permanent magnet (Fig. 2). The mechanical energy is then converted by the direct piezoelectric effect [13] into electric potential. As low frequency (LF) electromagnetic spectrum has an unlicensed band from 119-135 kHz, 130 kHz is considered for creating large volume low frequency magnetic fields to wirelessly transfer power to the piezoelectric energy harvesting system..

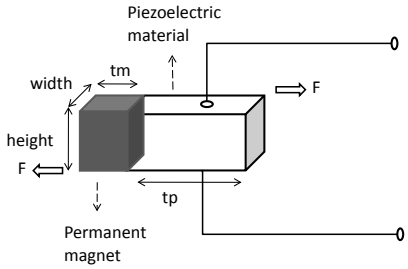

Fig. 2. Platinum cobalt coupled to the piezoelectric crystal.

The energy harvester, as shown in Fig. 3, can be formulated using a pair of electrical terminals and a pair of mechanical terminals. In this figure the entering charge and applied voltage at the electrical terminals are denoted by q and e, while the angular displacement and applied torque at the mechanical terminals are shown by θ and τ. This electromechanical conversion can be described by the following equation [14] in (1).

$$\begin{bmatrix} q \\ \theta \end{bmatrix} = \begin{bmatrix} C_{11} & C_{12} \\ C_{21} & C_{22} \end{bmatrix} \begin{bmatrix} e \\ \tau \end{bmatrix} \tag{1}$$

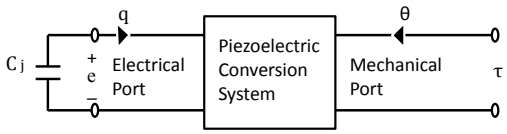

Fig. 3. Representation of a piezoelectric energy conversion system.

In (1) C_{11} is the input capacitance at the electrical port with zero torque applied to the mechanical port, C_{12} is the charge entering electrical port when it is short circuited and a torque is applied to mechanical port, C_{22} is the compliance at the mechanical port with a short circuit applied to the electrical port, and C_{21} is the displacement at mechanical port while a voltage is applied to the electrical port and no torque is applied to the mechanical one [15].

A. Magnetic field using a single turn circular planar coil

To create a magnetic field H(z) with frequency f at a distance z, a single turn circular planar coil of diameter $D = 2a$ of wire of diameter r has been considered, while the r.m.s current is flowing through the coil as shown in Fig. 4. Therefore the magnetic field at distance z is given by the relation (2).

$$H(z) = \frac{Ia^2}{2(a^2 + z^2)^{3/2}} \tag{2}$$

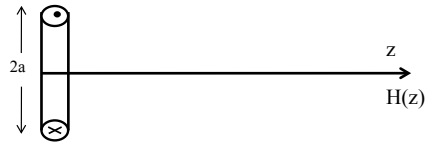

Fig. 4. Geometry of single turn coil.

B. Electrical power

As demonstrated in Fig. 3, when the conversion system is connected to an external load of C_j, it will have a charge q developed at electrical port when a torque is applied to the mechanical port. This charge is described by

$$q = -C_{11p}e \tag{3}$$

where C_{11p} for the slab piezoelectric material can be calculated by

$$C_{11p} = \frac{\varepsilon^T \varepsilon_0 wh}{t_p} \tag{4}$$

In the above equation ε^T is the relative dielectric constant under constant stress while t_p, w and h are thickness, width

and height of the piezoelectric plate, respectively. Solving the matrix for *e* gives

$$e = \frac{C_{12p}\tau_p}{C_{11p} + C_j} \tag{5}$$

By considering the dimensionless quantity $r = \frac{C_j}{C_{11}}$ then

$$e = \frac{C_{12p}\tau_p}{C_{11p}(1+r)} \tag{6}$$

Solving (1) by replacing relation (6) then gives,

$$\theta = \frac{C_{12p}\tau_p C_{21p}}{C_{11p}(1+r)} + C_{22p}\tau_p \tag{7}$$

Electromechanical coupling factor on piezoelectricity is noted by k^2 and defined as the ratio between the converted and total energy involved in a transformation cycle so:

$$k^2 = \frac{\text{Mechanical energy converd to stored electrical energy}}{\text{Mechanical energy input}} \tag{8}$$

In this piezoelectric conversion system k^2 can be defined by

$$k^2 = \frac{C_{12p}C_{21p}}{C_{11p}C_{22p}} \tag{9}$$

By using (9) and (7) we have

$$\theta = \left[1 - \frac{k^2}{1+r}\right] C_{22p}\tau_p \tag{10}$$

As a result the effective compliance for the capacitive loaded piezoelectric converter is given by

$$C_{22eff} = \frac{\theta}{\tau} = \left[1 - \frac{k^2}{1+r}\right] C_{22p} \tag{11}$$

where C_{22p} is the open circuit compliance at the electrical port. Observing that θ is proportional to τ, so the stored energy for a final torque applied to the mechanical port is given by

$$E_{MP} = \frac{1}{2}\left(1 - \frac{k^2}{1+r}\right) C_{22p}\tau^2 \tag{12}$$

Hence the electrical energy at the electrical port which will appear as stored energy in C_j is given by

$$E_{EP} = \frac{1}{2} C_j \left(\frac{{C_{12p}}^2}{{C_{11p}}^2(1+r)^2}\right)\tau^2 \tag{13}$$

By using (12) and (13)

$$\frac{E_{EP}}{E_{MP}} = \frac{rk^2}{(1+r)^2 - k^2(1+r)} \tag{14}$$

Therefore it can be proven that

$$K^2{}_{eff} = \frac{rk^2}{(1+r)^2 - k^2(1+r)} \tag{15}$$

C. Mechanical Power

The oscillating magnetic field provides the mechanical stress on the structure by the torque exerted on the permanent magnet as it is shown in Fig. 2. The r.m.s phasor T_s shows the magnitude of total torque on the harvesting structure.

$$T_s = \mu_0 vMH \tag{16}$$

In (16), μ_0 is permeability of free space, *v* is the volume of platinum cobalt (magnet) and *M* is the remnant magnetisation, in this equation the direction of the magnetisation *M* is orthogonal to magnetic field *H*.

The resulting energy E_{MS} of the structure flowing into the stiffness of the structure can be evaluated as

$$E_{MS} = |T_s|^2 C_{22s} \tag{17}$$

In (17) C_{22s} is the total compliance of the structure at the mechanical port. C_{22s} can be calculated by

$$C_{22s} = \frac{1}{\frac{1}{C_{22M}} + \frac{1}{C_{22eff}}} \tag{18}$$

In (18) C_{22M} is the compliance of magnet and obtained from

$$C_{22M} = \frac{S_M^E}{hwt_m} \tag{19}$$

where S_M^E is the compliance of the magnetic material. From the total mechanical stress placed on the structure, just the mechanical stress on the piezoelectric crystal will result to transferring electrical energy into stiffness of the piezoelectric as it is shown in

$$E_{MP} = \frac{1}{2}|T_p|^2 C_{22eff} \tag{20}$$

where $T_p = T_s\left(\frac{C_{22s}}{C_{22eff}}\right)$.

D. Mechanical Resonance and Quality factor

Resonance frequency plays a considerable role in energy outcome; as derived in (21). At the mechanical resonance frequency of the proposed structure with mechanical quality factor Q_m, the voltage generated at the electrical port is magnified by Q_m. Relation (21) gives the energy E_{EP} stored in C_j.

$$E_{EP} = {K_{eff}}^2 {Q_m}^2 E_{MP} \tag{21}$$

Substituting (20) while considering the fact that this energy is provided by a magnet with the magnetisation *M* and volume *v*, E_{EP} can be expressed by

$$E_{EP} = \frac{1}{2}{K_{eff}}^2 {Q_m}^2 \left(\mu_0 VM\right)^2 |H|^2 {C_{22s}}^2 \frac{1}{C_{22eff}} \tag{22}$$

Hence the energy flown into the capacitor C_j at the electrical port and the r.m.s voltage can be calculated as follows:

$$V_{EP}=\sqrt{\frac{1}{2}K_{eff}{}^{2}Q_m{}^{2}(\mu_0 VM)^2|H|^2C_{22s}{}^{2}\frac{1}{C_{22eff}C_j}} \qquad (23)$$

E. Numerical Analysis

The choice of piezoelectric material can have a considerable influence on the harvesting system performance. Since lead zirconate titanium known as PZT has the highest electromechanical coupling coefficient, this material is the most common type of piezoelectric used in power harvesting applications. Due to highest coupling coefficient and mechanical quality factor in the 1-5 modes the PZT-8 is chosen for the numerical evaluations.

As mentioned before, to ensure efficient transfer of energy in the magnetic field to electrical energy at the output port, it is vital to operate at resonant frequencies. From Fig. 5 it can be seen that a piezoelectric crystal of height 7 to 8 mm is required for the construction of the piezoelectric slab to achieve a resonance frequency of 130 kHz.

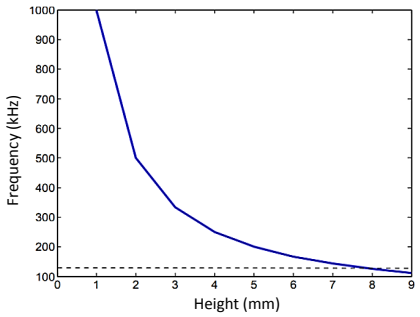

Fig. 5. Resonance frequency of PZT-8 with different heights.

This analysis has also been confirmed by ANSYS multiphysics modal analysis and the final results show, when the PZT-8 height is set to 7.5 mm, self-resonance is achieved at 129 kHz.

Based on (16) the magnetic material considered for the bar magnet should suitably have a high residual magnetisation *M*. Using PtCo (Platinum and Cobalt) based alloys, a residual magnetization *M* of 400,000 Am^{-1} is achievable.

As depicted in Fig. 2 following dimensions were used for the numerical analysis: w = 5 mm, t_p= 2 mm, t_m= 2 mm, and h = 7.5 mm. From Fig. 6 which is obtained from our numerical evaluation, it is demonstrated that the proposed energy harvesting system has the ability to generate up to 1.4 V.

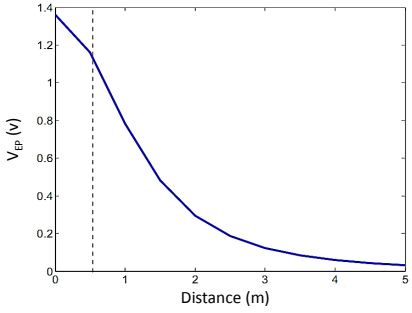

Fig. 6. V_{EP} at distance *z* from the coil.

IV. Simulation Results

Based on the analytical model, finite element modelling was performed in ANSYS Multiphysics for the magnetoelectric energy harvester. Similar dimensions to analytical model were used again for the simulation: w = 5 mm, t_p= 2 mm, t_m= 2 mm, and h = 7.5 mm.

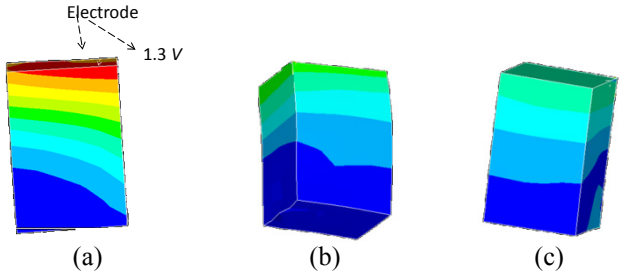

Fig. 7. Piezoelectric voltage distribution, (a) high voltage gain in resonance frequency, (b), (c) low voltage gain in 50 and 100 kHz frequencies.

According to the analytical calculations a 125 μN mechanical force exerted on the energy harvesting system at *z* = 0.5 m is applied in the simulation. Based on this mechanical force, a harmonic analysis was carried out for the proposed structure over a frequency range of 0 to 200 kHz in ANSYS Multiphysics. Fig. 8 depicts the electric potential vs. frequency relationship obtained from the simulations. As shown in Fig. 7 and Fig. 8, this system is capable of generating up to 1.3 V electric potential. Fig. 7 demonstrates voltage distribution in this system, the desired voltage is only obtained in Fig. 7 (a) which shows voltage distribution at resonance frequency.

Fig. 8 also indicates that the expected voltage from the device is almost negligible given the mechanical resonance does not occur. Hence it can be concluded that resonance frequency plays a vital role to achieve optimum power output from the proposed approach.

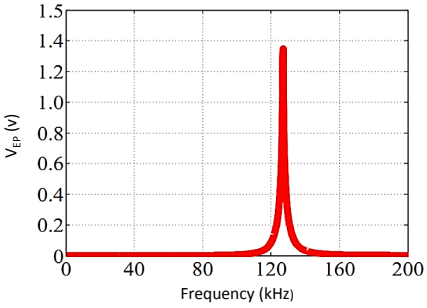

Fig. 8. Harmonic analysis of the output voltage of the energy harvester.

V. Application for Smart Implants

To demonstrate the potential of the proposed energy harvester, the resultant electric potential in the previous section is utilized to actuate a MEMS based biomedical micropump. Micropumps are miniaturized pumping devices fabricated by micromachining technologies [16]. They are generally categorized as mechanical or non-mechanical devices. The former typically has moving parts such as diaphragms and values. These parts demonstrates benefits in-terms of virtually non-restrictive fluid delivery and higher response rate over the latter [17].

Typical mechanical micropumps are displacement pumps comprised of a pump chamber closed by a flexible diaphragm as illustrated by Fig. 9. The fluid delivery is realized by the deflection of the diaphragm resulting in an over-pressure in the chamber, which drives the fluid out of the outlet. An under pressure causes the fluid to enter the chamber through the inlet. The pressure induced inside the chamber is a function of the change of volume known as the stroke volume, which is caused by the diaphragm deflection.

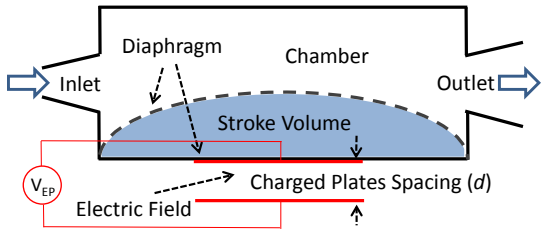

Fig. 9. An overview of a valveless electrostatically actuated micropump.

Over the years different schemes have been adopted for actuation of the diaphragm. These include but not limited to electrostatic, piezoelectric, thermopneumatic, bimetallic, shape memory alloy (SMA), ion conductive polymer film (ICPF), electromagnetic, and phase change type [16, 18]. Due to attractive benefits of electrostatic actuation such as fast response time and low power consumption, they have been of interest over the years [17]. In this section, after calculating the actuation force based on a predefined geometry, the actuation range of the diaphragm of a micropump is demonstrated by application of the equivalent force in a static structural simulation framework build in ANSYS. The structure of the valveless micropump is described in [12]. Here, the focus is on deflection of the diaphragm by the supplied electric potential from the magneto-electric energy harvester proposed in the previous section.

Electrostatic actuation is based on the Columbs attractive forces between charged plates. Using parallel plate approximation, the generated force between two plates can be described as [16]:

$$F = \frac{\varepsilon A E^2}{2d^2} \qquad (24)$$

Where F is the actuation force, ε is the permittivity of the dielectric between the two plates, A is the surface area of the plates, E the applied electric potential across the two plates and d is the spacing between them. Upon application of the electric potential (1 Volt), depending on the polarity, the charged plates enforce attractive or repelling forces upon each other. Geometrical and material properties of the proposed diaphragm model are summarized in TABLE I.

As demonstrated in Fig. 10, Silicon Nitride (Si3N4) is chosen for the midsection due to its high strength against bending, wear resistance and electrical insulation. The bottom of the midsection is coated with a thin layer of Aluminium alloy that represents the conductive plate associated with the diaphragm (Fig. 9). The attractive properties of low stiffness and biocompatibility, are some of the reasons for the increasing popularity of polymer based MEMS devices in recent years [19]. For the flexible part of the diaphragm Polyethylene has been chosen which makes actuation of the diaphragm feasible with the harvested potential described in Section IV.

TABLE I .

MATERIAL AND GEOMETRICAL PROPERTIES OF THE MICRODIAPHRAGM

Material Properties			
	Si_3N_4	Polyethylene	Al
Density (Kg/m^3)	3184	950	2770
Poisson's Ratio	0.24	0.42	0.33
Elastic Modulus (GPa)	169	1.1	71
Geometrical and Boundary Conditions			
Actuation Potential (V)		1 V	
Diaphragm Dimensions (W×L)		2×2 mm	
Diaphragm depth (H)		5 µm	
Midsection dimensions (W×L)		1×1 mm	
Diaphragm thickness (T_D)		2 µm	
Al coating thickness (T_{Al})		100 nm	

F. Simulation Results

To save time and computational resources the symmetry of the structure can be utilised, hence only one quarter of the diaphragm is modelled. The outer boundaries of the diaphragm are constrained in all directions. The derived force by substitution of values of TABLE I into relation (24) is applied as a pressure to the midsection of the model normal to its surface increased from 0 to the maximum pressure over 10 sub-steps as shown in Fig. 10. This figure also shows the contour plots of scaled deformation results of the diaphragm at the last sub-step.

Furthermore, Fig. 11 presents the minimum and maximum directional deflection of the midsection normal to the plane of the undeformed shape vs. pressure. These results are accompanied by maximum von-Mises stress distribution over midsection and flexible bodies vs. pressure curves.

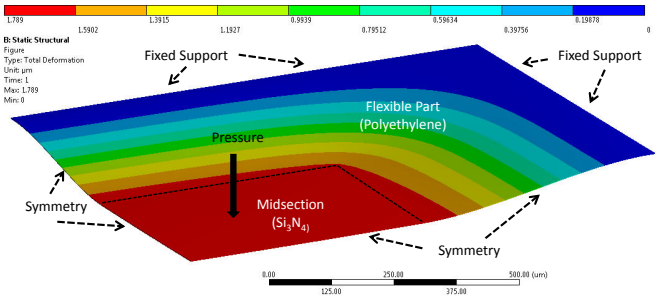

Fig. 10. Scaled deformation plots of quarter of the diaphragm, subject to the applied pressure, fixed support and symmetry boundary conditions.

Considering the maximum displacement value at the last sub-step (sub-step 10), clearly the distance between the charged plates (2 µm) is very well utilized while still providing a safe distance between them (≅0.2 µm) in order to avoid permanent adhesion of the plates. Moreover the von-Misses stress values indicates operation of the diaphragm well below the tensile strength of the constitutive materials, 15 MPa for polyethylene and 0.37 GPa for Silicon Nitride [20], ensuring safe operation of the diaphragm under electrostatic loads.

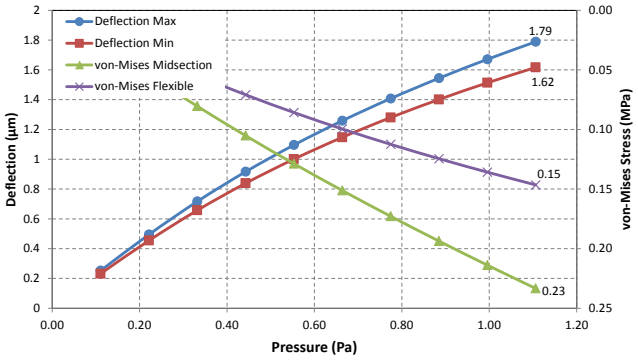

Fig. 11. Directional deformation of the midsection vs. applied pressure and, max von-Mises stress in the midsection and flexible parts vs. applied pressure.

The modelling results presented in this section demonstrate that the 1.3 V generated by the magneto-electric energy harvester is more than capable of meeting the required 1 V to successfully actuate the micropump presented in our analysis.

VI. Conclusion

With the increasing demand for micro-implants which are buried deep within body tissue, wireless and secure actuation of those devices has become a challenge. In this paper an alternative approach for remote powering of biomedical implants is proposed through integration of magnetic and electric physical domains interrelated by direct piezoelectric effect. The proposed energy harvesting system can potentially be integrated with a surface acoustic wave sensor using an input interdigitated transducer (IDT) to ensure the secure operation of the biomedical device. The output energy of the system is first calculated theoretically and then validated by numerical analysis.

To demonstrate the merit of system for actuation of MEMS devices, the harvested energy is then used to actuate the diaphragm of a mechanical micropump in an FEA framework. Our results indicate effectiveness of the energy harvester to deflect the diaphragm by about 1.8 µm while maintaining the safe operation conditions of the diaphragm. The resultant deflection utilizes about 24% of the chamber height for a stroke volume of 10% of the total chamber volume. A fully coupled methodology comprised of all the physics from the electromagnetic field to the structural mechanics and their interaction with the fluid domain accompanied with empirical studies is yet to be elaborated in our future works.

References

[1] J. A. Paradiso and T. Starner, "Energy scavenging for mobile and wireless electronics," *Pervasive Computing, IEEE,* vol. 4, pp. 18-27, 2005.

[2] M. Mohammadzaheri, S. Grainger, and M. Bazghaleh, "A comparative study on the use of black box modelling for piezoelectric actuators," *The International Journal of Advanced Manufacturing Technology,* vol. 63, pp. 1247-1255, 2012.

[3] M. Mohammadzaheri, S. Grainger, and M. Bazghaleh, "Fuzzy modeling of a piezoelectric actuator," *International Journal of Precision Engineering and Manufacturing,* vol. 13, pp. 663-670, 2012.

[4] S. Roundy and P. K. Wright, "A piezoelectric vibration based generator for wireless electronics," *Smart Materials and Structures,* vol. 13, pp. 1131-1142, 2004.

[5] M. J. Ramsay and W. W. Clark, "Piezoelectric energy harvesting for bio-MEMS applications," in *SPIE's 8th Annual International Symposium on Smart Structures and Materials*, 2001, pp. 429-438.

[6] S. R. Platt, S. Farritor, K. Garvin, and H. Haider, "The use of piezoelectric ceramics for electric power generation within orthopedic implants," *Mechatronics, IEEE/ASME Transactions on,* vol. 10, pp. 455-461, 2005.

[7] S. M. Allameh, O. Akogwu, M. Collinson, J. Thomas, and W. O. Soboyejo, "Piezoelectric generators for biomedical and dental applications: Effects of cyclic loading," *Journal of Materials Science: Materials in Medicine,* vol. 18, pp. 39-45, 2007.

[8] A. Pantelopoulos and N. G. Bourbakis, "A Survey on Wearable Sensor-Based Systems for Health Monitoring and Prognosis," *Systems, Man, and Cybernetics, Part C: Applications and Reviews, IEEE Transactions on,* vol. 40, pp. 1-12, 2010.

[9] R. Bashirullah, "Wireless Implants," *Microwave Magazine, IEEE,* vol. 11, pp. S14-S23, 2010.

[10] A. Yakovlev, D. Pivonka, T. Meng, and A. Poon, "A mm-sized wirelessly powered and remotely controlled locomotive implantable device," in *Solid-State Circuits Conference Digest of Technical Papers (ISSCC), 2012 IEEE International*, 2012, pp. 302-304.

[11] S. Kim, J. S. Ho, L. Y. Chen, and A. S. Y. Poon, "Wireless power transfer to a cardiac implant," *Applied Physics Letters,* vol. 101, p. 073701, 2012.

[12] D. W. E. Dissanayake, "Modelling and Analysis of Wirelessly Interrogated SAW based Micropumps for Drug Delivery Applications," Doctor of Philosophy, School of Electrical and Electronic Engineering, The University of Adelaide, 2009.

[13] D. Shen, *Piezoelectric energy harvesting devices for low frequency vibration applications*: ProQuest, 2009.

[14] P. H. Cole, "Coupling and quality factors in RFID," in *Proc. of Design, Charecterisation and Packaging for MEMS and Microelectronics*, 2001, pp. 1-11.

[15] D. C. Ranasinghe and P. H. Cole, "Evaluation of a MEMS based theft detection circuit for RFID labels," in *Proc. of VLSI Circuits and Systems II*, Seville, Spain, 2005, pp. 1110-1122.

[16] A. Nisar, N. Afzulpurkar, B. Mahaisavariya, and A. Tuantranont, "MEMS-based micropumps in drug delivery and biomedical applications," *Sensors and Actuators B: Chemical,* vol. 130, pp. 917-942, 2008.

[17] H. Gensler, R. Sheybani, P.-Y. Li, R. Mann, and E. Meng, "An implantable MEMS micropump system for drug delivery in small animals," *Biomedical Microdevices,* vol. 14, pp. 483-496, 2012.

[18] F. Amirouche, Y. Zhou, and T. Johnson, "Current micropump technologies and their biomedical applications," *Microsystem technologies,* vol. 15, pp. 647-666, 2009.

[19] N. C. Tsai and C. Y. Sue, "Review of MEMS-based drug delivery and dosing systems," *Sensors and Actuators A: Physical,* vol. 134, pp. 555-564, 2007.

[20] W. A. James F. Shackelford and W. Alexander, *CRC Materials Science and Engineering Handbook, Third Edition*: CRC PressINC, 2001.